• **Supplementary File** •

Distributed Sensor Network Localization Based on Local Bearing Measurement

Hao Zhang[1], Yunkai Lv[1], Zhuping Wang[1*], Zhian Zhan[1] & Huaicheng Yan[2]

[1]*Tongji University, Shanghai 200092, China;*
[2]*East China University of Science and Technology, Shanghai 200237, China*

Appendix A   Henneberg Construction [1, 2]

The directed graph $\mathcal{G} = (v, \varepsilon)$ consists of a pair of nodes v_j, v_k and a directed edge (v_k, v_j). A new directed graph $\mathcal{G}' = \{v', \varepsilon'\}$ is generated by adding a new node on the basis of graph $\mathcal{G}$ and performing the following steps:

1) Add free node

Connect a new node v_i with any two existing nodes v_j and v_k, then one has two directed edges (v_j, v_i) and (v_k, v_i), node v_i has two neighbor nodes v_j and v_k. In other words, free node v_i can receive the information transmitted by v_j and v_k.

2) Split directed edge

Vertex v_i has two neighbor nodes v_j and v_k in graph $\mathcal{G}$. Remove a directed edge (v_j, v_i) from the graph $\mathcal{G}$ and add a new free node v_m. Then two new directed edges (v_j, v_m) and (v_m, v_i) can be obtained.

An example of the Henneberg construction is shown in Fig. A1. The green dot represents the new sensor node, and the yellow edge is the new directed edges.
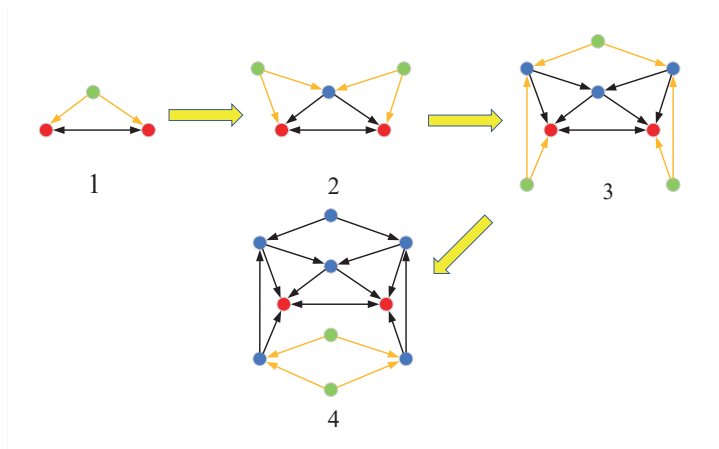
Figure A1   The Henneberg construction of directed graph.

Remark 1. Henneberg construction meets the conditions of bearing localizability [3] and the self-localizability [4] of sensor networks. In addition, Henneberg construction can be infinitely split in theory, which is suitable for large-scale sensor networks.

A directed acyclic leader-follower graph with ten vertices is shown in Fig. A2. The red vertex represents the anchor node with only one neighbor. The blue vertex is the free node with two neighbors. The n vertices sensor networks with directed graph $\mathcal{G} = (v, \varepsilon)$ obtained by a Henneberg construction is acyclic and rooted in-branching, which is bearing-localizable [1].

---

* Corresponding author (email: elewzp@tongji.edu.cn)
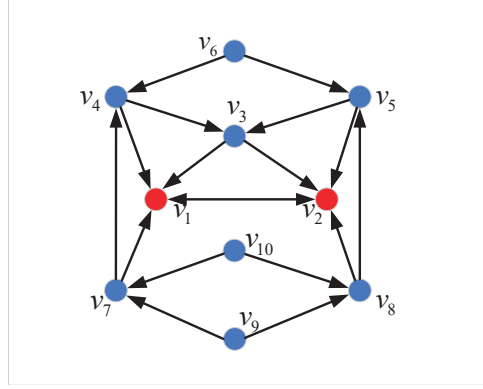
Figure A2 The directed acyclic leader-following graph with ten vertices.

Appendix B   Proof of lemma 1

An example of the local bearing measurements in two-dimensional Euclidean space is shown in Fig. B1.
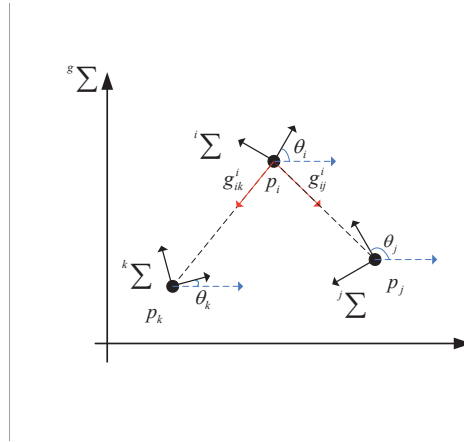
Figure B1 An example of the local bearing measurements.

In this work, the local bearing information g_{ik}^i and g_{ij}^i can be directly measured. Therefore, the accurate value of g_{jk}^i can be calculated by $g_{jk}^i = \frac{g_{ik}^i - g_{ij}^i}{\left\| g_{ik}^i - g_{ij}^i \right\|}$, where $\|\cdot\|$ stands for the 2-norm. Since $\hat{g}_{jk} = \hat{R}(\theta_i) g_{jk}^i$, one can obtain that $\dot{\hat{g}}_{jk} = \dot{\hat{R}}(\theta_i) g_{jk}^i$.

Define $\dot{\hat{g}}_{jk} = \left(\dot{\hat{x}}, \dot{\hat{y}} \right)^{\mathrm{T}}$, $\hat{g}_{jk} = (\hat{x}, \hat{y})^{\mathrm{T}}$ and $g_{jk}^i = (x_i, y_i)^{\mathrm{T}}$, then one has $\hat{R}(\theta_i) = \begin{bmatrix} x_i\hat{x} + y_i\hat{y} & \hat{x}y_i - x_i\hat{y} \\ -\hat{x}y_i + x_i\hat{y} & y_i\hat{y} + x_i\hat{x} \end{bmatrix}$, $\dot{\hat{R}}(\theta_i) = \begin{bmatrix} x_i\dot{\hat{x}} + y_i\dot{\hat{y}} & \dot{\hat{x}}y_i - x_i\dot{\hat{y}} \\ -\dot{\hat{x}}y_i + x_i\dot{\hat{y}} & y_i\dot{\hat{y}} + x_i\dot{\hat{x}} \end{bmatrix}$.

According to the above analysis, one can obtain that the orientation angle θ_i can be estimated indirectly by the estimated $\hat{g}_{jk}$. The proof of Lemma 1 is completed.

Appendix C   Proof of Theorem 1

Since the sensor network satisfies the Henneberg construction, the free node $i \in \{3, \cdots, n\}$ has two neighbors j and k, $1 \leqslant j \neq k \leqslant i - 1$.

The brief proof ideas are given as follows:

At first, we will prove that $\hat{R}(\theta_3)$ converges to $R(\theta_3)$ and $\hat{p}_3$ converges to p_3. Note that the two neighbors of free node 3 are anchor nodes 1 and 2. Then, we will prove that $\hat{R}(\theta_i)$ converges to $R(\theta_i)$ and $\hat{p}_i$ converges to p_i.

Proof.

Part I: the convergence analysis of free node 3.

The complete proof process of orientation estimation and position estimation of free node 3 are given as follows.

Step 1. The convergence of estimated rotation matrix $\hat{R}(\theta_3)$.

For free node 3, the equilibrium point of the estimation algorithm (1) satisfies the following condition

$$0 = -Q_{g_{12}} \hat{R}(\theta_3) g_{12}^3. \tag{C1}$$

Anchor nodes 1 and 2 know their absolute positions in $^g\sum$, so the unit vector g_{12} can be directly calculated without estimation.

By left multiplying the matrix $(\hat{g}_{12} - g_{12})^{\mathrm{T}}$ on both sides of (C1), one can obtain that

$$
\begin{aligned}
0 &= -(\hat{g}_{12} - g_{12})^{\mathrm{T}} Q_{g_{12}} \hat{R}(\theta_3) g_{12}^3 \\
&= -\left(\hat{R}(\theta_3) g_{12}^3 - g_{12}\right)^{\mathrm{T}} Q_{g_{12}} \left(\hat{R}(\theta_3) g_{12}^3 - g_{12} + g_{12}\right).
\end{aligned}
\tag{C2}
$$

Since $Q_{g_{12}} g_{12} = 0$, (C2) becomes

$$
0 = -\left(\hat{R}(\theta_3) g_{12}^3 - g_{12}\right)^{\mathrm{T}} Q_{g_{12}} \left(\hat{R}(\theta_3) g_{12}^3 - g_{12}\right).
\tag{C3}
$$

Equation (5) holds if and only if $\hat{R}(\theta_3) g_{12}^3 - g_{12} = 0$. In other words, the estimation algorithm (1) has a unique equilibrium point: $\hat{g}_{12} = g_{12}$.

Substitute $g_{12}^3 = R(\theta_3)^{-1} g_{12}$ into equation $\hat{R}(\theta_3) g_{12}^3 - g_{12} = 0$, one has

$$
\left(\hat{R}(\theta_3) - R(\theta_3)\right) g_{12} = 0.
\tag{C4}
$$

Denote $g_{12} = (x, y)^{\mathrm{T}}$, $\hat{R}(\theta_3) = \begin{bmatrix} \cos \hat{\theta}_3 & -\sin \hat{\theta}_3 \\ \sin \hat{\theta}_3 & \cos \hat{\theta}_3 \end{bmatrix}$ and $R(\theta_3) = \begin{bmatrix} \cos \theta_3 & -\sin \theta_3 \\ \sin \theta_3 & \cos \theta_3 \end{bmatrix}$, then (C4) becomes

$$
\begin{bmatrix} -2 \sin \frac{\hat{\theta}_3 + \theta_3}{2} \sin \frac{\hat{\theta}_3 - \theta_3}{2} & -2 \cos \frac{\hat{\theta}_3 + \theta_3}{2} \sin \frac{\hat{\theta}_3 - \theta_3}{2} \\ 2 \cos \frac{\hat{\theta}_3 + \theta_3}{2} \sin \frac{\hat{\theta}_3 - \theta_3}{2} & -2 \sin \frac{\hat{\theta}_3 + \theta_3}{2} \sin \frac{\hat{\theta}_3 - \theta_3}{2} \end{bmatrix} (x, y)^{\mathrm{T}} = 0.
\tag{C5}
$$

Since x and y are not equal to zero at the same time (such as $x = 0$, $y = 1$ or $y = 0$, $x = 1$), one has $\sin \frac{\hat{\theta}_3 + \theta_3}{2} \sin \frac{\hat{\theta}_3 - \theta_3}{2} = 0$ and $\cos \frac{\hat{\theta}_3 + \theta_3}{2} \sin \frac{\hat{\theta}_3 - \theta_3}{2} = 0$. Due to the fact that $\theta_3, \hat{\theta}_3 \in [0, 2\pi)$, a necessary and sufficient condition for the establishment of (C5) is $\hat{\theta}_3 = \theta_3$, that is, $\hat{R}(\theta_3) = R(\theta_3)$.

Based on the above analysis (C2)-(C5), one can conclude that the estimation algorithm (1) has a unique equilibrium point, and at the equilibrium point, $\hat{R}(\theta_3) = R(\theta_3)$.

Consider the Lyapunov function

$$
V = \frac{1}{2} \|\hat{g}_{12} - g_{12}\|^2.
\tag{C6}
$$

Let $\lambda_{Q_{g_{12}}}$ be the minimum eigenvalue of $Q_{g_{12}}$. Since $Q_{g_{12}}$ is a positive semidefinite matrix, $\lambda_{Q_{g_{12}}} \geqslant 0$. Then, one has

$$
\begin{aligned}
\dot{V} &= -\left(\hat{R}(\theta_3) g_{12}^3 - g_{12}\right)^{\mathrm{T}} Q_{g_{12}} \left(\hat{R}(\theta_3) g_{12}^3 - g_{12}\right) \\
&\leqslant -\lambda_{Q_{g_{12}}} \|\hat{g}_{12} - g_{12}\|^2 \\
&= -2\lambda_{Q_{g_{12}}} V.
\end{aligned}
\tag{C7}
$$

It follows from (C7) that the estimation algorithm (1) converges exponentially at the unique equilibrium point, and $\hat{R}(\theta_3)$ exponentially converge to $R(\theta_3)$.

Step 2. The convergence of estimated position $\hat{p}_3$.

For free node 3, the equilibrium point of the position estimation algorithm (2) satisfies

$$
0 = -Q_{\hat{g}_{31}}(\hat{p}_3 - p_1) - Q_{\hat{g}_{32}}(\hat{p}_3 - p_2).
\tag{C8}
$$

By left multiplying the matrix $(\hat{p}_3 - p_3)^{\mathrm{T}}$ on both sides of equation (C8), one has

$$
\begin{aligned}
0 &= -(\hat{p}_3 - p_3)^{\mathrm{T}} Q_{\hat{g}_{31}}(\hat{p}_3 - p_1) - (\hat{p}_3 - p_3)^{\mathrm{T}} Q_{\hat{g}_{32}}(\hat{p}_3 - p_2) \\
&= -(\hat{p}_3 - p_3)^{\mathrm{T}} Q_{\hat{g}_{31}}(\hat{p}_3 - p_3) - (\hat{p}_3 - p_3)^{\mathrm{T}} Q_{\hat{g}_{32}}(\hat{p}_3 - p_3) \\
&\quad + (\hat{p}_3 - p_3)^{\mathrm{T}} Q_{\hat{g}_{31}}(p_1 - p_3) + (\hat{p}_3 - p_3)^{\mathrm{T}} Q_{\hat{g}_{32}}(p_2 - p_3).
\end{aligned}
\tag{C9}
$$

According to Step 1, one can know that $\hat{g}_{31}$ converges to g_{31} and $\hat{g}_{32}$ converges to g_{32} after applying the estimation algorithm (1). Since $Q_{g_{ij}} g_{ij} = 0$, one can obtain that $Q_{\hat{g}_{31}}(p_1 - p_3) = 0$ and $Q_{\hat{g}_{32}}(p_2 - p_3) = 0$. Then, (C9) is equivalent to

$$
\begin{aligned}
0 &= -(\hat{p}_3 - p_3)^{\mathrm{T}} Q_{g_{31}}(\hat{p}_3 - p_3) - (\hat{p}_3 - p_3)^{\mathrm{T}} Q_{g_{32}}(\hat{p}_3 - p_3) \\
&= -(\hat{p}_3 - p_3)^{\mathrm{T}} (Q_{g_{31}} + Q_{g_{32}})(\hat{p}_3 - p_3).
\end{aligned}
\tag{C10}
$$

Equation (C10) holds if and only if $\hat{p}_3 - p_3 = 0$. Therefore, $\hat{p}_3 = p_3$ is the unique equilibrium point of the position estimation algorithm (2).

Consider the following Lyapunov function

$$
V = \frac{1}{2} \|\hat{p}_3 - p_3\|^2.
\tag{C11}
$$

According to (C9) and (C10), the derivative of (C11) is given as follows

$$
\begin{aligned}
\dot{V} &= -(\hat{p}_3 - p_3)^{\mathrm{T}} (Q_{g_{31}} + Q_{g_{32}})(\hat{p}_3 - p_3) \\
&\leqslant -\lambda_{Q_{g_{31}} + Q_{g_{32}}} \|\hat{p}_3 - p_3\|^2 \\
&= -2\lambda_{Q_{g_{31}} + Q_{g_{32}}} V,
\end{aligned}
\tag{C12}
$$

where $\lambda_{Q_{g31}+Q_{g32}}$ is the minimum eigenvalue of $(Q_{g31} + Q_{g32})$. Since Q_{g31} and Q_{g32} are positive semidefinite matrices, $\lambda_{Q_{g31}+Q_{g32}} \geqslant 0$.

From (C12), one can conclude that the position estimation algorithm (2) converges exponentially at the unique equilibrium point, and $\hat{p}_3$ exponentially converge to p_3.

Part II: the convergence analysis of free nodes 4 to n.

The complete proof process of the orientation estimation and the absolute position estimation of free node $i \in \{4, \cdots, n\}$ are shown below.

Step 1. The convergence of estimated rotation matrix $\hat{R}(\theta_i)$.

The equilibrium point of (1) satisfies

$$0 = -P_{\hat{g}_{jk}} \hat{R}(\theta_i) g_{jk}^i. \tag{C13}$$

By left multiplying the matrix $(\hat{g}_{jk} - g_{jk})^{\mathrm{T}}$ on both sides of (C13), one has

$$
\begin{aligned}
0 &= -(\hat{g}_{jk} - g_{jk})^{\mathrm{T}} Q_{\hat{g}_{jk}} \hat{R}(\theta_i) g_{jk}^i \\
&= -\left(\hat{R}(\theta_i) g_{jk}^i - g_{jk}\right)^{\mathrm{T}} Q_{\hat{g}_{jk}} \left(\hat{R}(\theta_i) g_{jk}^i - g_{jk} + g_{jk}\right).
\end{aligned} \tag{C14}
$$

Based on the analysis (C2) and (C3), one can know that $\hat{g}_{jk}$ can converge to g_{jk} when estimating the orientation angle of i, and due to the fact that $Q_{g_{jk}} g_{jk} = 0$, (C14) becomes

$$0 = -\left(\hat{R}(\theta_i) g_{jk}^i - g_{jk}\right)^{\mathrm{T}} Q_{\hat{g}_{jk}} \left(\hat{R}(\theta_i) g_{jk}^i - g_{jk}\right). \tag{C15}$$

It follows from (C15) that orientation estimation algorithm (1) has a unique equilibrium point $\hat{g}_{jk} = g_{jk}$, and $\hat{R}(\theta_i) = R(\theta_i)$ at this equilibrium point.

Select a Lyapunov function

$$V = \frac{1}{2} \|\hat{g}_{jk} - g_{jk}\|^2. \tag{C16}$$

The derivative of (C16) is shown as

$$
\begin{aligned}
\dot{V} &= -\left(\hat{R}(\theta_i) g_{jk}^i - g_{jk}\right)^{\mathrm{T}} Q_{\hat{g}_{jk}} \left(\hat{R}(\theta_i) g_{jk}^i - g_{jk}\right) \\
&\leqslant -\lambda_{Q_{\hat{g}_{jk}}} \|\hat{g}_{jk} - g_{jk}\|^2 \\
&= -2\lambda_{Q_{\hat{g}_{jk}}} V,
\end{aligned} \tag{C17}
$$

where $\lambda_{Q_{\hat{g}_{jk}}}$ represents the minimum eigenvalue of $Q_{\hat{g}_{jk}}$, and $\lambda_{Q_{\hat{g}_{jk}}} \geqslant 0$.

From (C17), one can conclude that (1) converges exponentially at the unique equilibrium point $\hat{g}_{jk} = g_{jk}$, and $\hat{R}(\theta_i)$ exponentially converge to $R(\theta_i)$ eventually.

Step 2. The convergence of estimated position $\hat{p}_i$.

The equilibrium point of (2) satisfies

$$0 = -Q_{\hat{g}_{ij}} (\hat{p}_i - \hat{p}_j) - Q_{\hat{g}_{ik}} (\hat{p}_i - \hat{p}_k). \tag{C18}$$

By left multiplying the matrix $(\hat{p}_i - p_i)^{\mathrm{T}}$ on both sides of (C18), one can obtain that

$$
\begin{aligned}
0 &= -(\hat{p}_i - p_i)^{\mathrm{T}} Q_{\hat{g}_{ij}} (\hat{p}_i - \hat{p}_j) - (\hat{p}_i - p_i)^{\mathrm{T}} Q_{\hat{g}_{ik}} (\hat{p}_i - \hat{p}_k) \\
&= -(\hat{p}_i - p_i)^{\mathrm{T}} Q_{\hat{g}_{ij}} (\hat{p}_i - p_i) - (\hat{p}_i - p_i)^{\mathrm{T}} Q_{\hat{g}_{ik}} (\hat{p}_i - p_i) \\
&\quad + (\hat{p}_i - p_i)^{\mathrm{T}} Q_{\hat{g}_{ij}} (\hat{p}_j - p_i) + (\hat{p}_i - p_i)^{\mathrm{T}} Q_{\hat{g}_{ik}} (\hat{p}_k - p_i).
\end{aligned} \tag{C19}
$$

In this work, the considered sensor network satisfies the Henneberg construction and nodes 1 & 2 are the anchor nodes, so the estimated orientation and position of free node 3 will converge first, and then gradually expand outward. Therefore, the estimated information $\hat{g}_{ij}$, $\hat{g}_{ik}$, $\hat{p}_j$ and $\hat{p}_k$ has converged to their true value when estimating the position of free node i. Based on the property of orthogonal projection matrix $Q_{g_{ij}} g_{ij} = 0$, one has $Q_{\hat{g}_{ij}} (\hat{p}_j - p_i) = 0$ and $Q_{\hat{g}_{ik}} (\hat{p}_k - p_i) = 0$.

According to the above analysis, (C19) is equivalent to

$$
\begin{aligned}
0 &= -(\hat{p}_i - p_i)^{\mathrm{T}} Q_{g_{ij}} (\hat{p}_i - p_i) - (\hat{p}_i - p_i)^{\mathrm{T}} Q_{g_{ik}} (\hat{p}_i - p_i) \\
&= -(\hat{p}_i - p_i)^{\mathrm{T}} \left(Q_{g_{ij}} + Q_{g_{ik}}\right) (\hat{p}_i - p_i).
\end{aligned} \tag{C20}
$$

From (C20), one can know that the unique equilibrium point of (2) is $\hat{p}_i = p_i$.

Design a Lyapunov function,

$$V = \frac{1}{2} \|\hat{p}_i - p_i\|^2. \tag{C21}$$

Based on the analysis from (C19) to (C20), the derivative of (C21) is given as follows

$$
\begin{aligned}
\dot{V} &= -(\hat{p}_i - p_i)^{\mathrm{T}} \left(Q_{\hat{g}_{ij}} + Q_{\hat{g}_{ik}}\right) (\hat{p}_i - p_i) \\
&\leqslant -\lambda_{Q_{\hat{g}_{ij}}+Q_{\hat{g}_{ik}}} \left\|Q_{\hat{g}_{ij}} + Q_{\hat{g}_{ik}}\right\|^2 \\
&= -2\lambda_{Q_{\hat{g}_{ij}}+Q_{\hat{g}_{ik}}} V,
\end{aligned} \tag{C22}
$$

where $\lambda_{Q_{\hat{g}_{ij}}+Q_{\hat{g}_{ik}}} \geqslant 0$ represents the minimum eigenvalue of the matrix $Q = Q_{\hat{g}_{ij}} + Q_{\hat{g}_{ik}}$. One can obtain that (2) converges exponentially at the equilibrium point $\hat{p}_i = p_i$, and $\hat{p}_i$ exponentially converges to p_i eventually.

The proof of Theorem 1 is completed.

Remark 2. In the proof of Theorem 1, the sensor network is regarded as a cascade system. The convergence of the orientation angle estimation information θ_i depends on the position information $\hat{p}_j$ and $\hat{p}_k$ of the neighbor nodes j and k, $1 \leqslant j \neq k \leqslant i-1$. Meanwhile, the convergence of the position estimation information of i depends on the accurate orientation angle estimation information $R(\theta_i)$. The proof of convergence starts from free node 3, and the neighbors of node 3 are anchor nodes 1 and 2 whose absolute positions are known. Therefore, the convergence of the orientation angle and the absolute position of the free nodes in the cascade system can be proved progressively using the Mathematical induction.

Appendix D   Simulation Examples

In this section, three simulation results are provided to illustrate the effectiveness of the proposed algorithms. The orientations of all free nodes are given randomly, and the absolute positions of all nodes satisfy the Henneberg construction.

In the simulation, only the local bearing measurements is used to align the orientation and estimate the absolute position. Compared with the distributed algorithm based on local bearing and relative orientation measurements [5], the relative orientation measurement is not needed. And it may be difficult to directly measure relative orientations in practice in the case of sensor node has no knowledge of global reference frame.

First, we consider a 10 nodes sensor network with directed acyclic graph generated by Henneberg construction. As shown in Fig. D1, the red circles are the anchor nodes, and the red-red lines represent the global reference frame of the anchor node. The blue circles are the free nodes, and the black-black lines indicate the local reference frames of the free node.
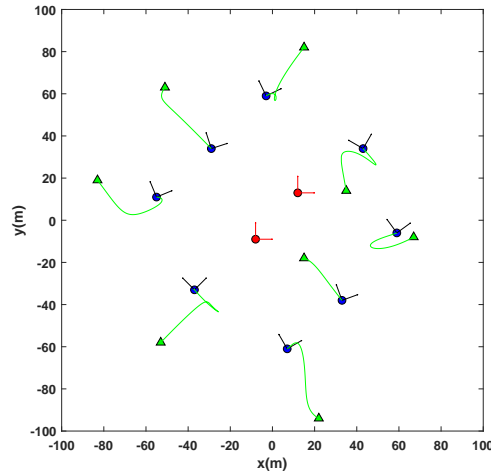
Figure D1   The convergence trajectories of the estimated positions of 8 free nodes.
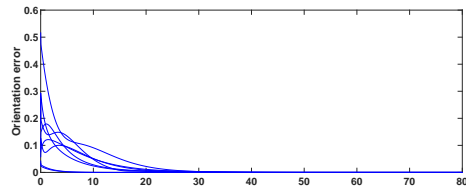
Figure D2   The orientation estimation error curves of 8 free nodes.
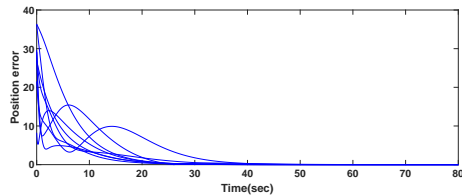
Figure D3   The position estimation error curves of 8 free nodes.

Applying the proposed estimation algorithms (1) and (2), the initial estimated values are given randomly, and the simulation results are shown in Figs. D1 - D3. The convergence trajectories of the free nodes are shown in Fig. D1, where the green triangles

are the initial estimated positions, the green curves represent the convergence process of the estimated positions. As can be seen in Fig. D2, the orientation estimation errors $\left\| \hat{R}\left(\theta_i\right) - R\left(\theta_i\right) \right\|$ of free nodes can converge to zero after 30 seconds. The position estimation errors $\|\hat{p}_i - p_i\|$ are shown in Fig. D3, one can find that after 40 seconds, the estimation position errors of the free nodes have converged to zero, which implies the effectiveness of the estimation algorithm (1) and (2). From Figs. D1-D3, one can conclude that the proposed estimation algorithms (1) and (2) can guarantee the accurate orientation and position estimation merely using the local bearing measurement.

Further, we also consider a new 18 nodes sensor network and a new 122 nodes sensor network, two of which are anchor nodes and the rest are free nodes. The new sensor network generated by adding new vertices and splitting edges, which is satisfies the Henneberg construction. Applying estimation algorithms (1) and (2), the convergence trajectories of the free nodes are shown in Figs. D4 -D5. It can be found that although the scale of sensor networks is increasing and the local orientation of free nodes is different from the anchor nodes, the proposed estimation algorithm (1) and (2) can still ensure that free nodes can estimate their absolute position in the global reference frame.
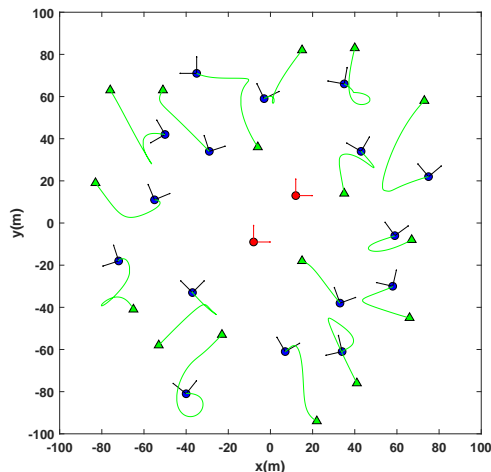
Figure D4   The convergence trajectories of the estimated positions of 16 free nodes.

Through the simulation results, one can draw the conclusions that: (a) the proposed estimation algorithms can realize the accurate orientation estimation and the absolute position localization of the sensor networks. (b) the proposed estimation algorithms are also applicable to large-scale sensor networks.

References

1   M. H. Trinh, S. Zhao, Z. Sun, et al. Bearing based formation control of a group of agents with leader-first follower structure, IEEE Transactions on Automatic Control, 2019, vol. 64, no. 2, pp. 598-613.
2   S. Zhao, D. Zelazo, Translational and scaling formation maneuver control via a bearing-based approach, IEEE Transactions on Control of Network Systems, 2017, vol. 4, no. 3, pp. 429-438.
3   P. Barooah, J. P. Hespanha, Estimation on graphs from relative measurements, IEEE Control Systems Magazine, 2007, vol. 27, no. 4, pp. 57-74.
4   Z. Lin, M. Fu, Y. Diao, Distributed self-localization for relative position sensing networks in 2D space, IEEE Transactions on Signal Processing, 2015, vol. 63, no. 14, pp. 3751-3761.
5   X. Li, X. Luo, S. Zhao, Globally convergent distributed network localization using locally measured bearings, IEEE Transactions on Control of Network Systems, 2019, vol. 7, no. 1, pp. 245-253.
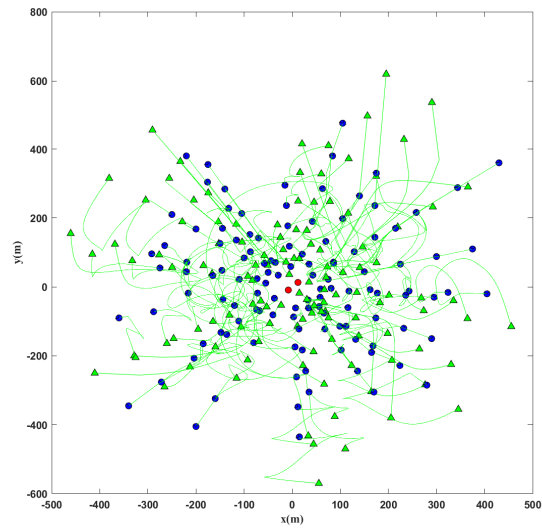
Figure D5 The position estimation error curves of 120 free nodes.